Soret and Dufour effects on MHD heat and mass transfer flow of a micropolar fluid over stretching sheet through porous medium with thermophoresis

Siva Gopal.R [#1], Prof.R.Siva Prasad[#2]
[#1]Research Scholar, Dept. of Mathematics, Sri Krishnadevaraya University, Anantapuramu–515003, A.P., India
[#2]Professor, Dept. of Mathematics, Sri Krishnadevaraya University, Anantapuramu – 515 003, A.P., India

ABSTRACT:

In this paper we analyzed the combined influence of Soret and Dufour effects on convective heat and mass transfer flow of a viscous electrically conducting micropolar fluid over a stretching sheet in the presence of suction/injection and thermophoresis particle deposition. The equation of non-linear momentum, micro-rotation, temperature and concentration along with the boundary conditions are solved by using finite element method.

1.Introduction

The theory of micropolar fluids has been an active area of research for several decades, because of its wide range of applications in analyzing fluid flow in brain, exotic lubricants, blood flow in animals, etc. Micropolar fluids are fluids with microstructure and related to the fluids with non-symmetrical stress tensor. They represent fluids consisting of rigid, randomly oriented or spherical particles suspended in a viscous medium, where the diformation of fluids particles is ignored(e.g. polymetricsuspentions, animal blood, liquid crystals). The theory of micropolar fluids was originally formulated by Eringen(8) by taking the local effects arising from the microstructure and the intrinsic motion of the fluid into the account. Micropolar fluids are non-Newtonian fluids consisting of dumb-bell molecules, colloidal fluids, liquid crystals, lubricants, suspension fluids, animal blood, etc. In this theory, the continuum is regarded as sets of structured particles which contain not only mass and velocity,but also a substructure. Bhargava et al. (4) have presented heat and mass transfer characteristics of micropolar fluid over porous stretching sheet. DamsehRebhi et al. (6) have noticed the influence of heat generation/absorption and first-order chemical reaction on micropolar fluid flow over a uniform stretching sheet. Yacos et al. (19) have reported boundary layer heat transfer stagnation-point flow of micropolar fluid over a stretching/shrinking sheet. Rosali et al. (16) analyzed micropolar fluid flow through porous media over a stretching/shrinking sheet with suction. Abd El-Aziz (1) studied boundary layer flow and heat transfer analysis of a micropolar fluid over a stretching sheet with viscous dissipation and found that thermal boundary layer thickness decelerates with the higher values of micropolar parameter. Mahmood et al. (9) have perceived boundary layer flow, heat transfer analysis of micropolar second grade fluid overa stretching sheet.

Thermophoresis is a phenomenon by which sub micron sized particles suspended in a non isothermal gas acquire a velocity relative to the gas in the direction of decreasing

temperature. The velocity acquired by the particle is known as the thermophoretic velocity and the force experienced by the suspended particles due to the temperature gradient is called the thermophoretic force. The magnitudes of the thermoporetic force and velocity are proportional to the temperature gradient. Thermophoresis has many applications in radioactive particle deposition in nuclear reactors, deposition of silicon thin films, particles impacting the blade surface of gas turbines and aerosol technology. Many authors have done good work by taking thermophoresis in the account. Seddeek (17)studied numerically the effect of variable viscosity and thermophoresis on a boundary layer flow with chemical reaction. Partha(12,13) analyzed the effects of Soret and Dufour with thermophoresis in a non-Darcy porous medium, later he extended the problem by taking suction/injection in to the account.

The effects Thermo-diffusion and Diffusion-thermo are very significant for the fluids which has higher temperature and concentration gradients. The Thermo-Diffusion (Soret) effect is corresponds to species differentiation developing in an initial homogeneous mixture submitted to a thermal gradient and the Diffusion-thermo (Dufour) effect corresponds to the heat flux produced by a concentration gradient. Usually, in heat and mass transfer problems the variation of density with temperature and concentration give rise to a combined buoyancy force under natural convection and hence the temperature and concentration will influence the diffusion and energy of the species. Alam et al. (2) have studied the Dufour and Soret effects on steady free convection and mass transfer flow past a semi-infinite vertical porous plate in a porous medium. Alam et al. (3) have investigated, the effect of suction on mixed convective flow along verticle plate by taking Soret and dufour effects. Dulal Pal et al. (7) has studied MHD non-Darcian mixed convection heat and mass transfer over a non-linear stretching sheet with Soret and Dufour effects and chemical reaction. MHD mixed convection flow with Soret and Dufour effects past a vertical plate embedded in porous medium was studied by Makinde (10).Reddy et al. (15) has presented finite element solution to the heat and mass transfer flow past a cylindrical annulus with Soret and Dufour effects.

2.Mathematical formulation

We consider two-dimensional, study, mixed convective heat and mass transfer flow of a viscous electricallyconducting, micropolar fluid through porous medium over a stretching sheet in the presence of thermophoresis, Soret and Dufour effects. The coordinate system is such that x-axis is taken along the stretching surface in the direction of the motion with the slot at origin, and the y-axis is perpendicular to the surface of the sheet as shown schematically in Fig. 1. A uniform transverse magnetic field (B_0) is applied along the y-axis. The stretching surface and the fluid are maintained same temperature and concentration initially,instantaneously they raised to a temperature$T_w(> T_\infty)$ and concentration $C_w(> C_\infty)$ which remain unchanged. The effects of thermophoresis are being taken in the diffusion equation to help in the understanding of the mass deposition variation on the surface. The temperature gradient in the y-direction is much larger than that in x-direction and hence thermophoretic velocity component normal to the surface is more importance.Under the above stated physical situations, the governing boundary-layer and Darcy-

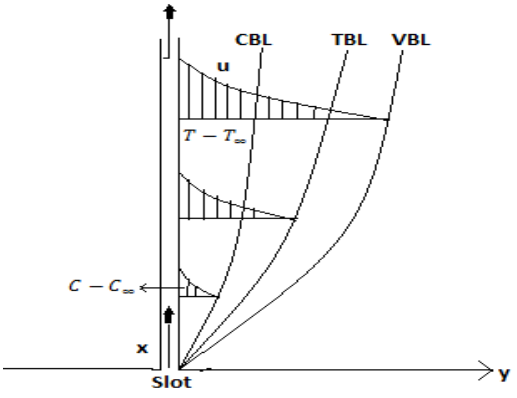

Fig. 1.Flow configuration and coordinate system.

Boussinesq's approximations, the basic equations are given by:

$$\frac{\partial u}{\partial x}+\frac{\partial v}{\partial y}=0 \quad (1)$$

$$u\frac{\partial u}{\partial x}+v\frac{\partial u}{\partial y}=\nu\frac{\partial^2 u}{\partial y^2}+k_1\frac{\partial W}{\partial y}+g_a\beta(T-T_\infty)+g_a\beta'(C-C_\infty)-\frac{\nu}{k_p}u+\frac{\sigma B_0^2}{\rho}u \quad (2)$$

$$u\frac{\partial W}{\partial x}+v\frac{\partial W}{\partial y}=-\frac{\kappa}{\rho J}\left(2W+\frac{\partial u}{\partial y}\right)+\frac{\gamma}{\rho J}\frac{\partial^2 W}{\partial y^2} \quad (3)$$

$$u\frac{\partial T}{\partial x}+v\frac{\partial T}{\partial y}=\alpha\frac{\partial^2 T}{\partial y^2}+\frac{\nu}{c_p}\left(\frac{\partial u}{\partial y}\right)^2+\frac{D_m k_T}{c_s c_p}\frac{\partial^2 C}{\partial y^2} \quad (4)$$

$$u\frac{\partial C}{\partial x}+v\frac{\partial C}{\partial y}=D_m\frac{\partial^2 C}{\partial y^2}+\frac{D_m k_T}{T_m}\frac{\partial^2 T}{\partial y^2}-\frac{\partial}{\partial y}(V_T C) \quad (5)$$

The associated boundary conditions on the vertical surface are defined as follows,

$$u=U_w(x)=ax,\quad v=V_1(x),\quad T=T_w,\quad C=C_w, W=-s\left(\frac{\partial u}{\partial y}\right),\quad at\ y=0.$$

$$u\to 0,\quad v\to 0,\quad T\to T_\infty,\quad C\to C_\infty,\ W=0,\quad at\ y\to\infty. \quad (6)$$

In the above equations *x* and y represents coordinate axis along the continuous surface in the direction of motion and perpendicular to it, *u* and *v* are the velocity components along *x* and y directions, respectively. The term $V_1=-\sqrt{\frac{\nu U_w}{2x}}V_0$ represents the mass transfer at the surface with $V_1<0$ for suction and $V_1>0$ for injection.

The effect of thermophoresis is usually prescribed by means of an average velocity acquired by small particles to the gas velocity when exposed to a temperature gradient. In boundary layer flow, the temperature gradient in y-direction is very much larger than in the *x*-direction and therefore only the thermophoretic velocity in *y*-direction is considered. As a consequence, the thermophoretic velocity V_T, which appears in Eq.(5), is expressed as

$$V_T=-\frac{k_1\nu}{T_r}\frac{\partial T}{\partial y} \quad (7)$$

in which k_1 is the thermophoretic coefficient and T_r is the reference temperature. A thermophoretic parameter τ is given by the relation

$$\tau=-\frac{k_1(T_w-T_\infty)}{T_r} \quad (8)$$

Where the typical values of τ are 0.01, 0.1and 1.0 corresponding to approximatevaluesof $-k_1(T_w-T_\infty)$ equal to 3, 30, 300Kfor a reference temperature of *T=300K.*

The mathematical analysis of the problem is simplified by introducing the following dimension less functions *f, h,* θ, φ and the similarity variable η

$$\eta=y\sqrt{\frac{a}{2\nu}},\ u=U_w\frac{df}{d\eta},\quad v=-\sqrt{\frac{\nu U_w}{2x}}f(\eta)+\frac{U_w y}{2x}\frac{df}{d\eta},$$

$$W=-\sqrt{\frac{U_w}{2\nu x}}U_w h,\theta(\eta)=\frac{T-T_\infty}{T_w-T_\infty},\quad \varphi(\eta)=\frac{C-C_\infty}{C_w-C_\infty}. \quad (9)$$

The continuity equation (1) is satisfied by the stream function $\psi(x, y)$ defined by

$$u=\frac{\partial\psi}{\partial y},\quad v=-\frac{\partial\psi}{\partial x} \quad (10)$$

Substituting Eqn. (9) in Eqns.(2) to (6), we obtain

$$f'''+B_1h'+ff''+G_r\theta+G_m\varphi-Kf'-Mf'=0 \quad (11)$$

$$\lambda h''-2\frac{\lambda}{G_1}(2h+f'')+f'h+fh'=0 \quad (12)$$

$$\theta''+\Pr f\theta'+\Pr Du\,\varphi''+\Pr Ec\,(f'')^2=0 \quad (13)$$

$$\varphi''+Sc\,f\,\varphi'+Sc\,Sr\,\theta''-\tau(\theta'\varphi'+\theta''\varphi)=0 \quad (14)$$

Where $\lambda = \frac{\gamma}{\rho\nu J}$ and $G_1 = \frac{\gamma a}{\nu\kappa}$ are micropolar parameters, $G_r = \frac{2g_a\beta x}{U_w{}^2}(T_w - T_\infty)$ is local Grashof number , $G_m = \frac{2g_a\beta' x}{U_w{}^2}(C_w - C_\infty)$ is local modified Grashof number , $B_1 = \frac{\kappa_1}{\nu}$ is the Coupling constant parameter, $K = \frac{U_w k_p}{2\nu x}$ is the permeability parameter, $Pr = \frac{\nu}{\alpha}$ is the Prandtl number, $Sc = \frac{\nu}{D_m}$ is the Schmidt number, $Du = \frac{D_m K_T}{c_s c_p \nu}\frac{(C_w - C_\infty)}{(T_w - T_\infty)}$ is the Dufour number, $Sr = \frac{D_m K_T}{\nu T_m}\frac{(T_w - T_\infty)}{(C_w - C_\infty)}$ is the Soret number, $Ec = \frac{U^2 w}{c_p}\frac{1}{(T_w - T_\infty)}$ is the Eckert number, $\nu = \frac{\mu + \kappa}{\rho}$ is the kinematic viscosity, $k_1 = \frac{\kappa}{\rho}(k_1 > 0)$ is the coupling constant, $M = \frac{2\sigma B_0^2 x}{\rho U_w}$ is the magnetic parameter. $\tau = -\frac{k_1(T_w - T_\infty)}{T_r}$ is the thermo phoretit parameter.

The corresponding transformed ***boundary conditions*** are

$f' = 1, f = V_0, h = -sf'', \theta = 1, \varphi = 1,$ at $y = 0$

$f' = 0, h = 0, \theta = 0, \varphi = 0$ at $y \to \infty$ (15)

Where $f(0) = V_0$ with $V_0 < 0$ and $V_0 > 0$ corresponding to injection and suction respectively.

The major physical quantities of interest in this problem are the local skin friction coefficient C_f , the local Nusselt number Nu_x and the local Sherwood number Sh_x are defined, respectively, by

$C_f = \frac{f''(0)}{Re_x{}^{\frac{1}{2}}}$, $Nu_x = -\frac{\theta'(0)}{Re_x{}^{\frac{1}{2}}}$, $Sh_x = -\frac{\varphi'(0)}{Re_x{}^{\frac{1}{2}}}$.

3. Method of solution

The finite- element method (FEM) has been implemented to obtain numerical solutions of coupled non-linear equations (11) to (14) of third-order in f and second order in h, θ, φ under boundary conditions (15).This technique is extremely efficient and allows robust solutions of complex coupled, nonlinear multiple degree differential equation systems.The details of finite-element method can find in Bhargava et al. (4), Rana et al. (14). The steps in volved in this method are as follows.

(i) Finite-element discretization

In the finite element discretization the entire interval is divided into a finite number of subintervals and this subinterval is called an element. The set of all these elements is called the finite-element mesh.

(ii) Generation of the element equations

a. Variational formulation of the mathematical model over the typical element (an element from the mesh) is performed.
b. An approximate solution of the variational problem is assumed, and the element equations are made by substituting this solution in the above system.
c. Using interpolating polynomials the stiffness matrix is constructed.

(iii) Assembly of element equations

By imposing inter element continuity conditions all the algebraic equations are assembled. This result a large number of algebraic equations called global finite-element model and it represents the whole domain.

(iv) Imposition of boundary conditions

The boundary conditions which represent the flow model are imposed on the assembled equations.

(v) Solution of assembled equations

The assembled equations so obtained can be solved by any of the numerical techniques, namely, the Gauss elimination method, LU decomposition method, etc. An important consideration is that of the shape functions which are employed to approximate actual functions.

For the solution of system non-linear ordinary differential equation (11) – (14) together with boundary conditions (15) , first we assume that

$$\frac{\mathrm{df}}{\mathrm{d\eta}} = \mathrm{j} \tag{16}$$

The equations (11) to (14) then reduces to

$$j'' + B_1 h' + f j' + G_r\theta + G_m\varphi - (K+M)j = 0 \tag{17}$$

$$\lambda h'' - 2\frac{\lambda}{G_1}(2h + j') + jh + fh' = 0 \tag{18}$$

$$\theta'' + \mathrm{Pr}\, f\, \theta' + \mathrm{Pr}\, Du\, \varphi'' + \mathrm{Pr}\, Ec\, (j')^2 = 0 \tag{19}$$

$$\varphi'' + Sc\, f\, \varphi' + Sc\, Sr\, \theta'' - \tau(\theta'\varphi' + \theta''\varphi) = 0 \tag{20}$$

The boundary conditions take the form

$$j = 1, f = V_0, h = -sj', \theta = 1, \varphi = 1, \quad \text{as } y = 0$$
$$j = 0, h = 0, \theta = 0, \varphi = 0, \quad \text{as} y \to \infty \tag{21}$$

3.2. Variational formulation

The variational form associated with Eqs. (16) to (20) over a typical linear element (η_e, η_{e+1}) is given by

$$\int_{\eta_e}^{\eta_{e+1}} w_1 \left(\frac{\mathrm{df}}{\mathrm{d\eta}} - \mathrm{j}\right) \mathrm{d\eta} = 0 \tag{22}$$

$$\int_{\eta_e}^{\eta_{e+1}} w_2 \left(j'' + B_1 h' + f j' + G_r\theta + G_m\varphi - (K+M)j \right) \mathrm{d\eta} = 0 \tag{23}$$

$$\int_{\eta_e}^{\eta_{e+1}} w_3 \left(\lambda h'' - 2\frac{\lambda}{G_1}(2h + j') + jh + fh'\right) \mathrm{d\eta} = 0 \tag{24}$$

$$\int_{\eta_e}^{\eta_{e+1}} w_4 \left(\theta'' + \mathrm{Pr}\, f\, \theta' + \mathrm{Pr}\, Du\, \varphi'' + \mathrm{Pr}\, Ec\, (j')^2\right) \mathrm{d\eta} = 0 \tag{25}$$

$$\int_{\eta_e}^{\eta_{e+1}} w_5 \left(\varphi'' + Sc\, f\, \varphi' + Sc\, Sr\, \theta'' - \tau(\theta'\varphi' + \theta''\varphi)\right) \mathrm{d\eta} = 0 \tag{26}$$

Where w_1, w_2, w_3, w_4 and w_5 are arbitrary test functions and may be viewed as the variations in *f, h, θ,* and ϕ, respectively.

3.3. Finite- element formulation

The finite-element model may be obtained from above equations by substituting finite-element approximations of the form

$$f = \sum_{j=0}^{2} f_j \Psi_j,\ j = \sum_{j=0}^{2} j_j \Psi_j,\ h = \sum_{j=0}^{2} h_j \Psi_j,\ \theta = \sum_{j=0}^{2} \theta_j \Psi_j,\ \phi = \sum_{j=0}^{2} \phi_j \Psi_j \tag{27}$$

With $w_1 = w_2 = w_3 = w_4 = w_5 = \Psi_i, \quad (i = 1,2).$

Where Ψ_i are the shape functions for a typical element (η_e, η_{e+1}) and are defined as

$$\Psi_1^e = \frac{(\eta_{e+1} - \eta)}{(\eta_{e+1} - \eta_e)}, \qquad \Psi_2^e = \frac{(\eta - \eta_e)}{(\eta_{e+1} - \eta_e)}, \qquad \eta_e \le \eta \le \eta_{e+1}. \tag{28}$$

The finite element model of the equations thus formed is given by

$$\begin{bmatrix} [K^{11}] & [K^{12}][K^{13}] & [K^{14}][K^{15}] \\ [K^{21}] & [K^{22}][K^{23}] & [K^{24}][K^{25}] \\ [K^{31}] & [K^{32}][K^{33}] & [K^{34}][K^{35}] \\ [K^{41}] & [K^{42}][K^{43}] & [K^{44}][K^{45}] \\ [K^{51}][K^{52}][K^{53}] & [K^{54}][K^{55}] \end{bmatrix} \begin{bmatrix} f \\ j \\ h \\ \theta \\ \phi \end{bmatrix} = \begin{bmatrix} \{r^1\} \\ \{r^2\} \\ \{r^3\} \\ \{r^4\} \\ \{r^5\} \end{bmatrix}$$

Where $[K^{mn}]$ and $[r^m]$ (m, n = 1, 2, 3, 4,5) are defined as

$K_{ij}{}^{11} = \int_{\eta_e}^{\eta_{e+1}} \psi_i \frac{\partial \psi_j}{\partial \eta} d\eta$, $K_{ij}{}^{12} = -\int_{\eta_e}^{\eta_{e+1}} \psi_i \psi_j \, d\eta$, $K_{ij}{}^{13} = K_{ij}{}^{14} = K_{ij}{}^{15} = 0.$

$K_{ij}{}^{21} = \int_{\eta_e}^{\eta_{e+1}} \psi_i \frac{\partial \psi_j}{\partial \eta} \, d\eta$, $K_{ij}{}^{22} = -\int_{\eta_e}^{\eta_{e+1}} \frac{\partial \psi_i}{\partial \eta}\frac{\partial \psi_j}{\partial \eta} d\eta + (M+K)\int_{\eta_e}^{\eta_{e+1}} \psi_i \psi_j d\eta$,

$K_{ij}{}^{23} = B_1 \int_{\eta_e}^{\eta_{e+1}} \psi_i \frac{\partial \psi_j}{\partial \eta} d\eta$, $K_{ij}{}^{24} = G_r \int_{\eta_e}^{\eta_{e+1}} \psi_i \psi_j \, d\eta$, $K_{ij}{}^{25} = G_m \int_{\eta_e}^{\eta_{e+1}} \psi_i \psi_j \, d\eta.$

$K_{ij}{}^{31} = \int_{\eta_e}^{\eta_{e+1}} \psi_i \frac{\partial \psi_j}{\partial \eta} \, d\eta$, $K_{ij}{}^{32} = 2\frac{\lambda}{G_1}\int_{\eta_e}^{\eta_{e+1}} \psi_i \frac{\partial \psi_j}{\partial \eta} \, d\eta + \int_{\eta_e}^{\eta_{e+1}} \psi_i \psi_j d\eta.$

$$K_{ij}{}^{33} = \lambda \int_{\eta_e}^{\eta_{e+1}} \psi_i \frac{\partial \psi_j}{\partial \eta} d\eta + 4\frac{\lambda}{G_1}\int_{\eta_e}^{\eta_{e+1}} \psi_i \psi_j d\eta, K_{ij}{}^{34} = K_{ij}{}^{35} = 0.$$

$K_{ij}{}^{41} = Pr \int_{\eta_e}^{\eta_{e+1}} \psi_i \frac{\partial \psi_j}{\partial \eta} \, d\eta$, $K_{ij}{}^{42} = Pr.Ec \int_{\eta_e}^{\eta_{e+1}} \psi_i \frac{\partial \psi_j}{\partial \eta}\frac{\partial \psi_j}{\partial \eta} \, d\eta, K_{ij}{}^{43} = 0,$

$$K_{ij}{}^{44} = \int_{\eta_e}^{\eta_{e+1}} \psi_i \bar{\theta} \frac{\partial \psi_j}{\partial \eta} \, d\eta, K_{ij}{}^{45} = \Pr Du \int_{\eta_e}^{\eta_{e+1}} \psi_i \bar{\phi} \frac{\partial \psi_j}{\partial \eta} \, d\eta,$$

$K_{ij}{}^{51} = Sc \int_{\eta_e}^{\eta_{e+1}} \psi_i \bar{\phi} \, \psi_j \, d\eta$, $K_{ij}{}^{52} = 0$, $K_{ij}{}^{53} = 0,$

$K_{ij}{}^{54} = Sc \, Sr \int_{\eta_e}^{\eta_{e+1}} \psi_i \bar{\theta} \frac{\partial \psi_j}{\partial \eta} \, d\eta - \tau \int_{\eta_e}^{\eta_{e+1}} \psi_i \bar{\theta} \frac{\partial \psi_j}{\partial \eta} \psi_j d\eta \, K_{ij}{}^{55} =$

$\int_{\eta_e}^{\eta_{e+1}} \frac{\partial \psi_i}{\partial \eta}\frac{\partial \psi_j}{\partial \eta} \, d\eta - \tau \int_{\eta_e}^{\eta_{e+1}} \psi_i \frac{\partial \psi_j}{\partial \eta} d\eta.$

$r_i^2 = 0, r_i^2 = -\left(\psi_i \frac{d\Psi_i}{d\eta}\right)_{\eta_e}^{\eta_{e+1}}$, $r_i^3 = -\left(\psi_i \frac{d\Psi_i}{d\eta}\right)_{\eta_e}^{\eta_{e+1}}$, $r_i^4 = -\left(\psi_i \frac{d\Psi_i}{d\eta}\right)_{\eta_e}^{\eta_{e+1}}, r_i^5 = -\left(\psi_i \frac{d\Psi_i}{d\eta}\right)_{\eta_e}^{\eta_{e+1}}$

Where

$\bar{f} = \sum_{j=0}^{2} f_i \frac{\partial \Psi_i}{\partial \eta}$, $\bar{J} = \sum_{j=0}^{2} j_i \frac{\partial \Psi_i}{\partial \eta}$, $\bar{h} = \sum_{j=0}^{2} h_i \frac{\partial \Psi_i}{\partial \eta}, \bar{\theta} = \sum_{j=0}^{2} \theta_i \frac{\partial \Psi_i}{\partial \eta}$, $\bar{\phi} = \sum_{j=0}^{2} \phi_i \frac{\partial \Psi_i}{\partial \eta}.$

The very important aspect in this numerical procedure is to select an approximate finite value of η_∞. So, in order to estimate the relevant value of η_∞, the solution process has been started with an initial value of $\eta_\infty = 4$, and then the equations (22) – (26) are solved together with associated boundary conditions. We have updated the value of η_∞ and the solution process is continued until the results are not affected with further values of η_∞.The choice of $\eta_{max} = 4$ for velocity and temperature and $\eta_{max} = 6$ for concentration have confirmed that all the numerical solutions approach to the asymptotic values at the free stream conditions.

4. Grid Independence Test

To investigate the sensitivity of the solutions to mesh density, we have performed the grid in variance test for velocity, temperature and concentration distributions and are shown in table 1. It is observed from this table that in the same domain the accuracy is not affected, even the number of elements increased, by decreasing the size of the elements.

5. Results and discussion

Comprehensive numerical computations were conducted for different values of the parameters and results are illustrated graphically as well as in tabular form. Selected computations are presented in Figs. 2-21. The correct ness of the current numerical method is checked with the results obtained by Mohanty et al. (11) .

Fig.2 illustrates the variation of velocity profiles for various values of suction parameter V_0. It is observed from this figure that the velocity decreases with increase in the value of the suction parameter. This is because of the reality that the momentum boundary layer thickness depreciates with increment in V_0. Further, it is seen that the velocity decreases with increase in η till it satisfies the boundary condition at $\eta = \infty$. Fig.3 illustrates the effect of V_0 on micro-rotation profiles. Since there is no buoyancy term occurs in the angular momentum equation, then there exist strong coupling between translational velocity and micro-rotation fields. The linear momentum equation(11) also contains the micro-rotation term, which further gives coupling between velocity and angular velocity fields. All the profiles have different values at $\eta = 0$ because of the initial condition $h(0) = -sf''(0)$which is always non-zero since $s = 0.5$ and $f''(0) \neq 0$.The effect of V_0 on temperature profiles (θ) is shown in Fig.4. It is seen from this figure that temperature profiles decreases with increase in the values ofV_0. This is due to the fact that the presence of wall suction has the tendency to reduce the thermal boundary layer thickness which results the reduction in the temperature profiles. Fig.5 depicts the changes in concentration profiles for different values of suction parameter V_0. This figure indicates that increase in suction parameter V_0 decreases concentration profiles and is because of the imposition of suction/injection parameter into the flow region depreciate the concentration of the specius in the solutal boundary layer. Therefore, From the above Figs. 2 - 5 we observed that the imposition of wall fluid suction (V_0>0) in the present problem of flow has the effect of depreciating the velocity, micro-rotation, temperature and concentration boundary layer thicknesses at every finite value of η.The decelaration in all profiles with the higher values of suctionparameter (V_0>0) is from the reality that suction is taken away the warm fluid from the fluid region.

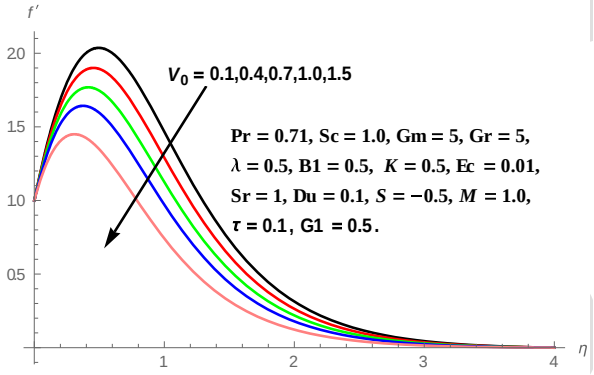

Fig. 2.Effect of V_0 on Velocity profile.

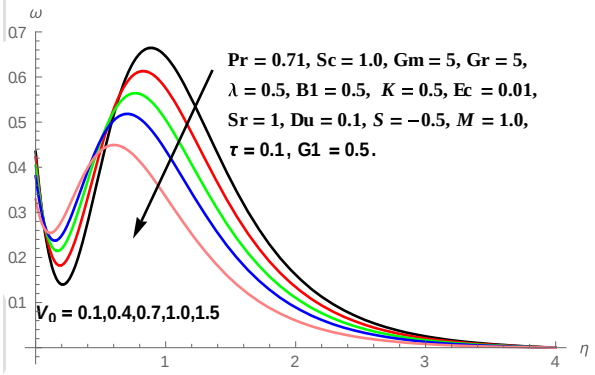

Fig. 3.Effect of V_0 on Micro-rotation profile.

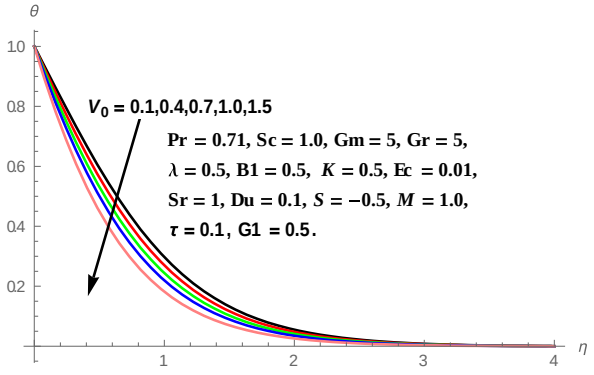

Fig. 4.Effect of V_0 on temperature profile.

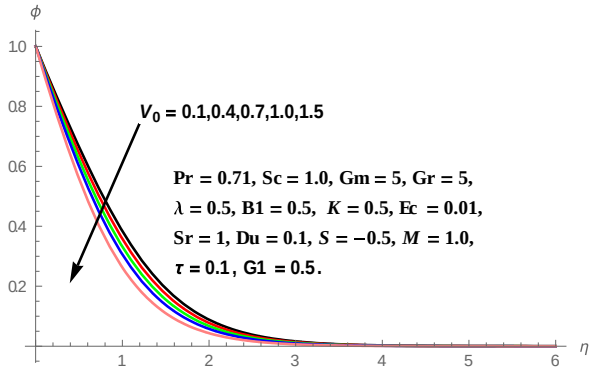

Fig. 5.Effect of V_0 on Concentration profile.

The combined impact of *Sr* and *Du* on velocity, microrotation, temperature and concentration profiles is depicted in Figs. 6-9. In these graphs *Sr* and *Du* values are taken as *Sr*= 0.5,0.8,1.1,1.4,1.8 and *Du* = 0.5,0.3,0.2,0.15,0.1. It is noticed that the velocity and angular velocity of the fluid rises with the rising values of *Sr* and *Du* in the boundary layer regime. It is clearly observed from these graphs that the temperature distributions decreases whereas concentration profiles increases at all points in the flow field with the increasing values of Soret parameter (*Sr*) and the decreasing values of Dufour parameter (*Du*).This is because of the fact that the diffusive species with higher values of Soret parameter (*Sr*) has the tendency of increasing concentration profileswhereas thermal species with lower Dufour parameter (*Du*) values has the tendency of depreciating temperature profilesin the flow field.Thus, it is concluded from Figs. 8-9 that the temperature and concentration distributions are more influenced with the values of Soret and Dufour parameters.

The variations in velocity, microrotation, temperature and concentration distributions for various values of thermophoretic parameter τ is depicted in Figs.10-13 We noticed depreciation in the velocity and microrotation profiles with the increasing values of thermophoretic parameter (τ). It is seen from fig.10 that the thickness of the thermal boundary layer increases in flow region with higher values of thermophoretic parameter τ. This is because of the fact that the particles near the hot surface create a thermophoretic force causes the increment in the thermal boundary layer thickness.However, the thickness of solutal boundary layersdepriciatesin the entire flow region with increase in the values of thermophoreticparameter τ.

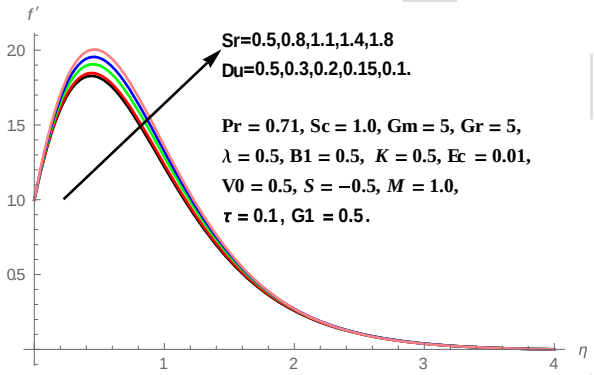

Fig.6. Effect of *Sr* & *Du* on Velocity profile.

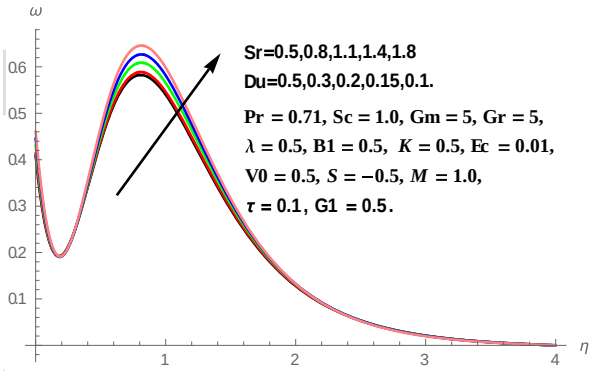

Fig.7.Effect of *Sr* & *Du* on Microrotation profile.

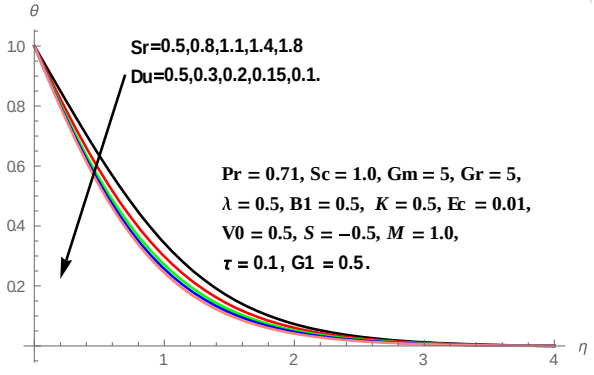

Fig.8.Effect of *Sr* & *Du* on Temperature profile.

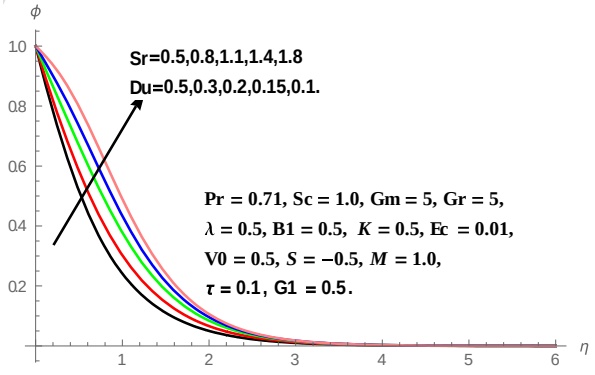

Fig.9.Effect of *Sr* & *Du* on concentration profile.

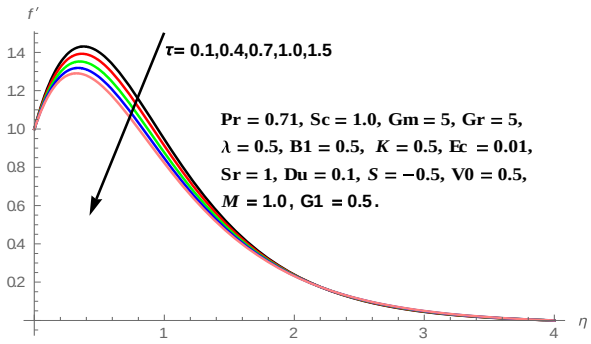

Fig.10.Effect of τ on Velocity profile.

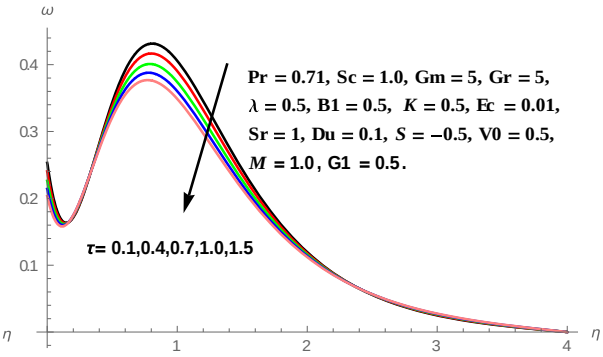

Fig.11.Effect of τ on Microrotation profile.

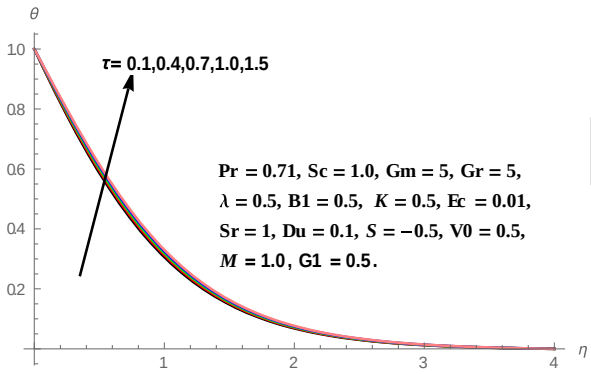

Fig. 12.Effect of τ on Temperature profile.

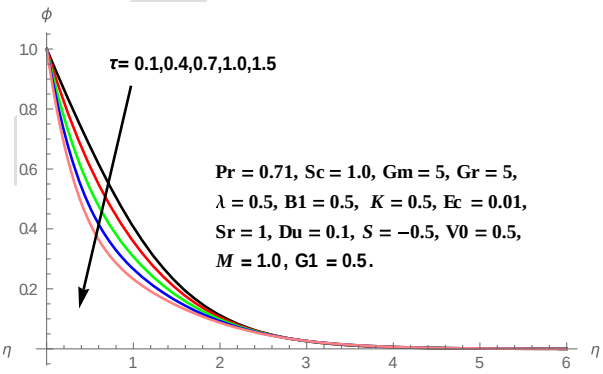

Fig. 13.Effect of τ on Concentration profile.

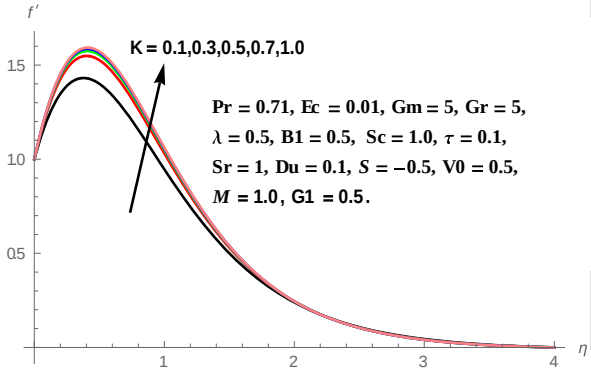

Fig.14.Effect of K on Velocity profile.

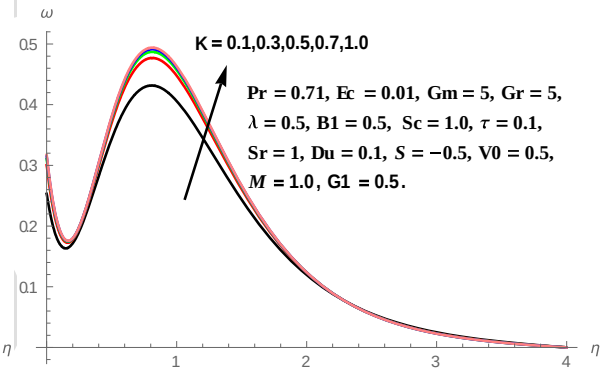

Fig.15.Effect of K on Microrotation profile.

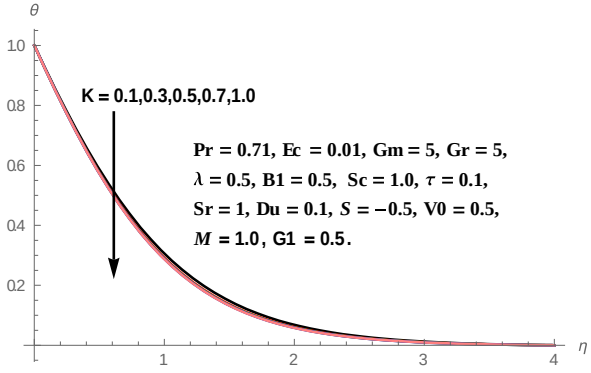

Fig.16.Effect of K on Temperature profile.

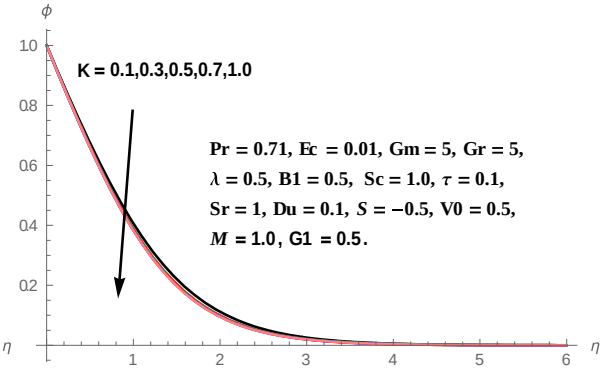

Fig.17.Effect of K on Temperature profile.

The impact of porous parameter (*K*) on hydrodynamic, angular, thermal and solutal boundary layers is plotted in Fig.14-17.

The impact of porous parameter (*K*) on hydrodynamic, angular, thermal and solutal boundary layers is plotted in Fig.14-17. It is observed that the velocity and microrotation profiles are both elevates with the higher values of porous parameter (K). The thickness of thermal boundary layer and concentration boundary layer is depreciates as the values of (K) increases.

The impact of Schdmith number (*Sc*) on hydrodynamic, angular, thermal and solutal boundary layers is plotted in Fig.18-21. The velocity and microrotation profiles are both deteriorates with the higher values of (*Sc*). The thermal boundary layer thickness is elevated where as the concentration boundary layer thickness is diminishes.R with increasing values of (*Sc*).

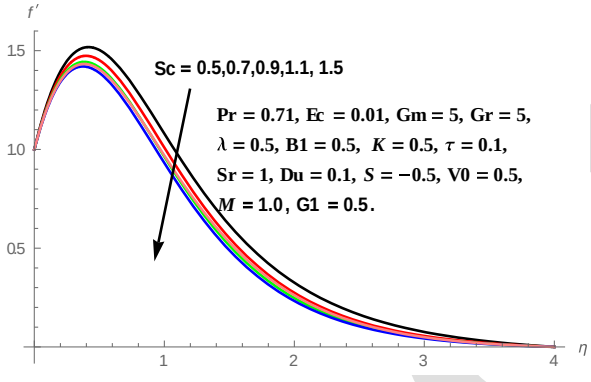

Fig.18.Effect of *Sc* on Velocity profile.

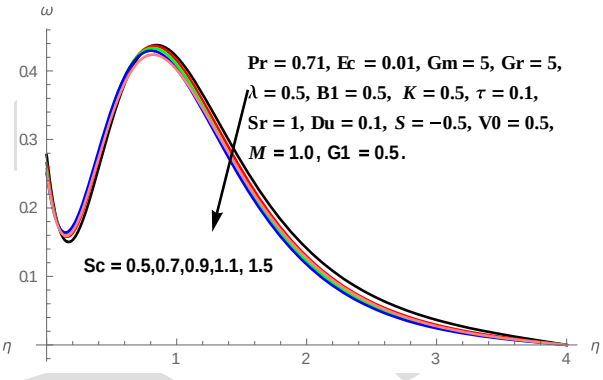

Fig.19.Effect of *Sc* on Microrotation profile.

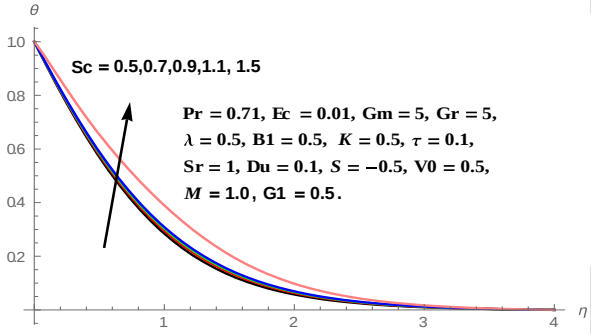

Fig.20.Effect of *Sc* on Temperature profile.

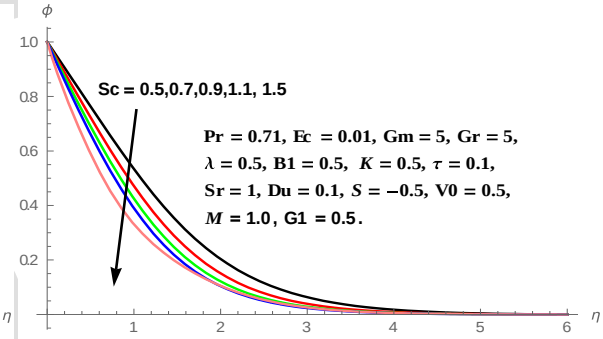

Fig.21.Effect of *Sc* on concentration profile.

The variation of local skin-friction co-efficient $f''(0)$, local Nusselt number $-\theta'(0)$, and local Sherwood number $-\phi'(0)$ for different values of suction parameter (V_0) is presented in table 1. It is seen from table that the local skin-friction co-efficient depreciates whereas the dimensionless heat and mass transfer rates elevates with increase in suction parameter (V_0). The combined influence of *Sr* and *Du* on skin-friction coefficient, Nusselt number and sherwood number is also reported in table 1. It is noticed that $f''(0)$ and the dimensionless heat transfer rates are both improved whereas the dimentionless mass transfer rates falls with the increasing values of *Sr* and decreasing values of *Du*. It is evident from table 1 that the skin-friction co-efficient and Nusselt number depreciates where as Sherwood number enhances with the increasing values of thermophoresis parameter (τ).

Table 1. The local Skin-friction, Nusselt number and Sherwood number for different values of the important parameters.

V_0	Sr	Du	τ	$f''(0)$	$-\theta'(0)$	$-\varphi'(0)$
0.1	1.0	0.1	0.1	4.341664	0.840417	0.713787
0.4	1.0	0.1	0.1	4.217637	0.957082	0.766098
0.7	1.0	0.1	0.1	4.035646	1.081757	0.820302
1.0	1.0	0.1	0.1	3.797455	1.214205	0.877212
0.5	1.0	0.1	0.1	2.531069	0.926322	0.689786
0.5	0.5	0.5	0.1	4.073383	0.743463	1.165773
0.5	0.8	0.3	0.1	4.130123	0.897880	0.960502
0.5	1.1	0.2	0.1	4.304030	0.985056	0.688923
0.5	1.4	0.1	0.1	4.304302	1.025185	0.482014
0.5	1.0	0.1	0.1	2.531069	0.926322	0.689786
0.5	1.0	0.1	0.4	2.403028	0.899578	0.967457
0.5	1.0	0.1	0.7	2.262505	0.867547	1.307852
0.5	1.0	0.1	1.0	2.140653	0.837243	1.637596
0.5	1.0	0.1	0.1	2.531069	0.926322	0.689786

6. Conclusions

In the present analysis we have investigated the combined influence of suction and thermophoresis on the mixed convective heat and mass transfer boundary layer flow of a micropolar fluid through porous medium over a stretching sheet in the presence of Thermo-Diffusion and Diffusion-Thermo effects. Similarity transformations are used to transform the resulting partial differential equations in to the set of highly non-linear ordinary differential equations and are solved numerically by using Finite element method. The most significant findings of the present study are as follows.

- The thickness of hydrodynamic, microrotation, thermal and solutal boundary layers is reduced with the higher values of suction parameter (V_0). This is because of the fact that suction is taken away the warm fluid from the fluid region.
- The thermal boundary layer thickness is improved with the increasing values of thermophoretic parameter (τ). This is because of the fact that thermophoresis acts against temperature gradient, so that, the particles move from the region of higher temperature to the region of lower temperature.
- The rates of non-dimentionless temperaturedecreases with an increase in the values of Soret number *Sr*.
- The rates of non-dimentionless concentration improves with an increasing values of Soretparameter*Sr*.
- TheNusslet number increases with an increase in the values of Dufour number *Du*.

7. References

1. Abd El-Aziz, M. (2013): Mixed convection flow of a micropolar fluid from an unsteady stretching surface with viscous dissipation, J. Egypt. Math. Soc., Vol. 21, pp. 385–394.
2. Alam, M.S., Ferdows,M., Ota, M. and Maleque, M.A. (2006a): Dufour and Soret effects on steady free convection and mass transfer flow past a semi-infinite vertical porous plate in a porous medium,Int. J. Appl. Mech. Eng., Vol. 11, pp. 535–545.
3. Alam, M.S. and Rahman, M.M. (2006b): Dufour and Soret effects on mixed convection flow past a vertical porous flat plate with variable suction, Non Linear Analysis; Modelling and Control, Vol. 11, pp. 3-12.

4. Bhargava, R., Kumar, L. and Takhar, H.S. (2003): Finite element solution of mixed convection microploar fluid driven by a porous stretching sheet, Int. J. Eng. Sci., Vol. 41, pp. 2161–2178.
5. Bhargava, R., Sharma, R and Bég, O.A. (2009): Oscillatory chemically-reacting MHD free convection heat and mass transfer in a porous medium with Soret and Dufour effects, finite element modeling, Int. J. Appl. Math. Mech, Vol, 5, pp. 15–37.
6. Damseh Rebhi, a., Al-Odat, M.Q., Chamkha, A.J. and ShannakBenbella, A. (2009): Combined effect of heat generation or absorption and first-order chemical reaction on micropolar fluid flows over a uniformly stretched permeable surface, Int. J. Therm. Sci., Vol. 48, pp. 1658–1663.
7. Dulal Pal. and Mondal, H. (2011): MHD non-Darcian mixed convection heat and mass transfer over a non-linear stretching sheet with Soret and Dufour effects and chemical reaction, International communications in heat and mass transfer, Vol.38, pp. 463-467.
8. Eringen, A.C. (1996): Theory of micropolar fluids, J. Math. Mech, Vol.16, pp.1-18.
9. Mahmood, R., Nadeem, S. and Akber, N.S. (2013): Non-orthogonal stagnation point flow of a micropolar second grade fluid towards a stretching surface with heat transfer, J. Taiwan Inst.Chem. Eng., Vol. 44, pp. 586–595.
10. Makinde, O.D. (2011): On MHD mixed convection with soret and dufour effects past a vertical plate embedded in a porous medium, Latin American Applied Research, Vol. 41, pp. 63-68.
11. Mohanty, B., Mishra, S.R. and Pattanayak, H.B. (2015): Numerical investigation on heat and mass transfer effect of micropolar fluid over a stretching sheet through porous media, Alexandria Engineering Journal, Vol. 54, pp. 223–232.
12. Partha, M.K. (2008): Thermophoresis particle deposition in a non-Darcy porous medium under the influence of Soret, Dufour effects, Heat and Mass Transfer, Vol. 44, pp. 969-977.
13. Partha, M.K. (2009): Suction/injection effects on thermophoresis particle deposition in a non-Darcy porous medium under the influence of Soret and Dufour effects, Int. J. Heat Mass Transfer, Vol. 52, pp. 1971-1979.
14. Rana, P., and R. Bhargava (2012): Flow and heat transfer of a Nano fluid over a nonlinearly stretching sheet: a numerical study, Comm. Nonlinear Sci. Numer. Simulat, Vol.17,pp. 212–226.
15. Reddy, P.S., and Rao. V.P. (2012): Thermo-diffusion and diffusion –thermo effects on convective heat and mass transfer through a porous medium in a circular cylindrical annulus with quadratic density temperature variation – Finite element study,Journal of Applied Fluid Mechanics, Vol, 5, pp. 139-144.
16. Rosali, H., Ishak, A. and Pop, I. (2012): Micropolar fluid flow towards a stretching/shrinking sheet in a porous medium with suction, Int. Commun. Heat Mass Transf. Vol. 39, pp. 826–829.
17. Seddeek, M.A. (2005): Finite element method for the effects of chemical reaction, variable viscosity, thermophoresis and heat generation/absorption on a boundary layer hydromagnetic flow with heat and mass transfer over a heat surface, ActaMechanica, Vol. 177, pp. 1-18.
18. Seini, Y.I. and Makinde, O.D. (2013):Hydromagnetic flow with dufour and soret effects past a vertical plate embedded in porous media, Mathematical Theory and Modelling, 2013.
19. Yacos, N.A., Ishak, A. and Pop, I. (2011): Melting heat transfer in boundary layer stagnation-point flow towards a stretching/shrinking sheet in a micropolar fluid, Comput. Fluids, Vol. 47, pp. 16–21.